

Article

Agro-Industrial Waste of Malt Bagasse: Perspectives on the Development of Eco-Friendly Ceramic Material

João Pedro da Silva Costa Andrade ¹, Daiane Cecchin ^{1,*} , Carlos Maurício Fontes Vieira ², Geovana Carla Girondi Delaqua ², Flávio Castro da Silva ¹, Leonardo da Silva Hamacher ¹, Tulane Rodrigues da Silva ², Mugahed Amran ^{3,4} , Juliana Lobo Paes ⁵ , Cristina Moll Hüther ¹ , Dirlane de Fátima do Carmo ¹  and Afonso Rangel Garcez de Azevedo ^{1,6} 

¹ Department of Agricultural Engineering and Environment, Federal Fluminense University, Street Passo da Pátria, 156, Niterói 24210-240, RJ, Brazil; joaoandrade@id.uff.br (J.P.d.S.C.A.); flavioacastro@id.uff.br (F.C.d.S.); lshamacher@id.uff.br (L.d.S.H.); cristinahuther@id.uff.br (C.M.H.); dirlanefc@id.uff.br (D.d.F.d.C.); afonso@uenf.br (A.R.G.d.A.)

² Advanced Materials Laboratory, State University of the Northern Rio de Janeiro, Avenue Alberto Lamego, 2000, Campos dos Goytacazes 28013-602, RJ, Brazil; vieira@uenf.br (C.M.F.V.); geovanagironi@gmail.com (G.C.G.D.); tulanerodrigues@gmail.com (T.R.d.S.)

³ Department of Civil Engineering, College of Engineering, Prince Sattam Bin Abdulaziz University, Alkharj 11942, Saudi Arabia; mugahed_amran@hotmail.com

⁴ Department of Civil Engineering, Faculty of Engineering and IT, Amran University, Amran 9677, Yemen

⁵ Department of Engineering, Rural University of Rio de Janeiro, Rio de Janeiro 23890-000, RJ, Brazil; juliana.lobop@gmail.com

⁶ Civil Engineering Laboratory, State University of the Northern Rio de Janeiro, Avenue Alberto Lamego, 2000, Campos dos Goytacazes 28013-602, RJ, Brazil

* Correspondence: daianececchin@id.uff.br



Citation: Andrade, J.P.d.S.C.; Cecchin, D.; Vieira, C.M.F.; Delaqua, G.C.G.; Silva, F.C.d.; Hamacher, L.d.S.; da Silva, T.R.; Amran, M.; Paes, J.L.; Moll Hüther, C.; et al. Agro-Industrial Waste of Malt Bagasse: Perspectives on the Development of Eco-Friendly Ceramic Material. *Sustainability* **2023**, *15*, 9120. <https://doi.org/10.3390/su15119120>

Academic Editors: Teodor Rusu and Antonio Zuorro

Received: 14 April 2023

Revised: 31 May 2023

Accepted: 1 June 2023

Published: 5 June 2023



Copyright: © 2023 by the authors. Licensee MDPI, Basel, Switzerland. This article is an open access article distributed under the terms and conditions of the Creative Commons Attribution (CC BY) license (<https://creativecommons.org/licenses/by/4.0/>).

Abstract: The construction sector is increasingly seeking sustainable alternatives in its processes worldwide, with a particular focus on the production of eco-friendly materials. Additionally, the improper disposal of solid waste is rapidly increasing, particularly in the agro-industry, including the waste generated from beer processing such as malt bagasse. Therefore, the objective of this study was to incorporate malt bagasse residue into ceramic materials at varying proportions (0, 2.5, 5, 10, and 15%) as a partial substitute for clay, submitted to different sintering temperatures (750, 850, 950, and 1050 °C). The raw materials, namely ceramic mass and malt bagasse, were characterized based on their chemical properties (XRF, loss of fire, and elemental analysis), physical properties (grain size, Atterberg limits), and mineralogical properties (XRD) characteristics. The properties of the ceramics, both with and without the incorporation of waste, were evaluated using dilatometry, apparent density, apparent porosity, water absorption, linear shrinkage, and tensile strength. The compositions that exhibited the best sintering temperatures were subjected to microstructural characterization using optical microscopy and X-ray diffraction (XRD). Significant differences were observed in the properties of the ceramic material, particularly in terms of linear shrinkage and apparent porosity. It was concluded that as the amount of malt bagasse residue incorporated increased, the mechanical properties of the pieces decreased. The incorporation of 15% residue resulted in the lowest performance, primarily due to a greater loss of mass. However, it should be noted that the incorporation of up to 5% malt bagasse for all the studied temperatures can still be considered acceptable, as it meets the minimum recommended value of 1.5 MPa for masonry ceramic components. This incorporation of malt bagasse contributes to both the technological and environmental aspects of civil construction.

Keywords: malt bagasse; ceramic; alternative materials; sustainability

1. Introduction

Currently, the utilization of residues from the agro-industry and food industry has gained prominence in the implementation of more sustainable techniques across various

sectors, including the civil construction sector [1]. These industries contribute significantly to the generation and disposal of solid waste, as well as to the emission of greenhouse gases, particularly carbon dioxide CO₂ [2]. Among the solid waste produced, the by-products of brewing production, such as grains and malt bagasse, account for approximately 85% of the brewery waste [3]. Malt bagasse specifically represents approximately 20 kg of bagasse for every 100 L of beer produced [4]. Countries such as China, the United States, Brazil, Mexico, and Germany are leaders in annual beer production, with Brazil ranking among the top 20 countries with an average consumption of 64 L per person per year [5,6].

Despite the significant amounts of by-products generated by brewing production and the potential for their reuse, their disposal, particularly in landfills, has resulted in various negative impacts [6]. This has necessitated a transition towards new sustainable guidelines, particularly in terms of the economy and circular production [7]. These challenges are further amplified by limited resources, logistics issues, and solid waste management, as well as the need to optimize the valorization of biomass generated by breweries [6]. Consequently, numerous studies have been conducted within the brewing industry to enhance the efficiency and sustainability of its technologies, production processes, and utilization of by-products [8–11]. Notably, studies utilizing malt bagasse have garnered attention [12–14] due to its low cost and attractive technological properties [14].

In a study conducted by Quaranta et al. [15], the viability of using malt bagasse as a pore-forming material in the production of ceramic bricks was evaluated. The researchers found that clay mixtures containing 10% malt bagasse residue exhibited favorable physical and mechanical properties. The values for porosity, modulus of rupture, volumetric variation, and weight loss were deemed suitable for application. Stefani et al. [16] investigated the properties of thermoplastic composites produced using post-consumer polypropylene fibers and malt bagasse (MB) from the brewing industry. They varied the malt bagasse fiber contents between 0, 10, 20, and 30%, as well as the concentrations of a coupling agent (CA), namely 0, 1, 3, 5, and 7%. The authors observed that the sample with 30% MB fibers exhibited 44% less deformation compared to the other samples, indicating superior mechanical resistance. However, it also had the highest water absorption. The composite with a fiber content of 30% MB and 3% CA was selected due to its modulus of elasticity, which was 10.3% higher than the same composite without CA. This finding demonstrated the feasibility of using malt bagasse as reinforcement in this type of composite.

In a study conducted Cordeiro et al. [12], the thermal behavior of malt bagasse and its heat capacity were examined through calorimetry. The researchers analyzed samples with varying moisture contents (50, 40, 30, 20, and 15%). They assessed the content of volatiles, fixed carbon, and ash present in the residue, considering that the thermal degradation of malt bagasse occurs in two stages: moisture release and organic matter decomposition. The calorific value of malt bagasse was found to vary with decreasing moisture and density, exhibiting a high percentage of volatile materials and low percentages of ash and carbon. Ferreira et al. [13] studied biodegradable composites composed of cassava starch blended with different agro-industrial residues, including sugarcane bagasse and corn straw, malt bagasse, or orange bagasse. The authors used a cassava starch solution as a binder and observed that all composites exhibited high water sorption capacity when stored under high or medium humidity. Mechanical analyses indicated that the addition of different amounts of agro-industrial residues made the composites stiffer, although they were more susceptible to degradation. Nevertheless, the authors concluded that the utilized waste materials held potential for producing biodegradable composites.

Moreover, the construction sector has been actively seeking alternatives to enhance its environmental performance, as it is recognized as one of the sectors with a significant impact on the environment [7]. In this regard, recent studies focused on the incorporation of solid waste into construction materials [17,18], including the utilization of biomass residues in ceramic materials [15,19]. However, the objective of this study was to assess the impact of incorporating varying percentages of malt bagasse in ceramic material. It is worth noting

that malt bagasse has received limited attention in the research of alternative construction materials due to its unique biomass characteristics.

2. Materials and Methods

This experimental work was conducted at the Universidade Estadual do Norte Fluminense Darcy Ribeiro—UENF, situated in Campos dos Goytacazes, RJ. The research was carried out on the premises of the Laboratory of Advanced Materials (LAMAV) and the Laboratory of Civil Engineering (LECIV).

2.1. Materials

For this research, the following raw materials were utilized (Figure 1a): ceramic mass (ball clay + sand) sourced from the region of Campos dos Goytacazes, RJ, and malt bagasse residue (Figure 1b) obtained from a brewery located in Niterói, RJ.

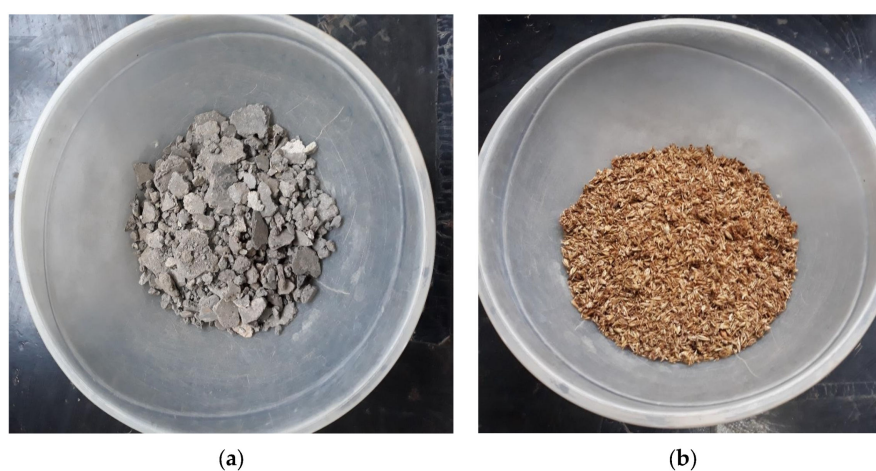


Figure 1. Raw materials used in the study: (a) clay (ball clay); (b) malt residue (source: author's personal collection).

Clay and sand were obtained from Arte Cerâmica Sardinha, located in Campos dos Goytacazes, RJ. They were collected using a shovel and stored in plastic bags until they were transported to LAMAV/LECIV for sample preparation. The malt residue, obtained fresh, was directly collected from a brewery in Niterói, RJ, after the brewing process. The residue was stored in plastic containers with lids and refrigerated at approximately 3 °C to preserve its organic nature during transported to UENF.

After collection, the ceramic mass samples were subjected to several processing steps. First, they were homogenized and dried in an oven at a temperature of approximately 110 °C for approximately 24 h. Following the drying process, the samples were disaggregated using a jaw crusher and further crushed using a porcelain mortar and pestle. Sieving was then performed using a 20-mesh sieve to obtain powdered material for the granulometry test, following the guidelines of NBR (Brazilian Standard) 7181 [20]. Additionally, a 40-mesh sieve was used to determine the consistency limits according to NBR 7181 and NBR 7180 [21]. A portion of the sample was also passed through a 200-mesh sieve for chemical and mineralogical characterization of the material.

The malt bagasse was initially subjected to a drying process to eliminate excess moisture. It was dried in an oven at 70 °C for 96 h. Subsequently, the residue underwent an additional drying step for 24 h at 60 °C to remove any remaining moisture. Given the high humidity and organic nature of malt bagasse, specific drying conditions were necessary. After the drying process, the malt bagasse was ground using a mortar and pestle until it passed through a 40-mesh sieve.

Once the raw materials were prepared and processed, they were allocated to the respective stages of the experimental schedule, as depicted in Figure 2.

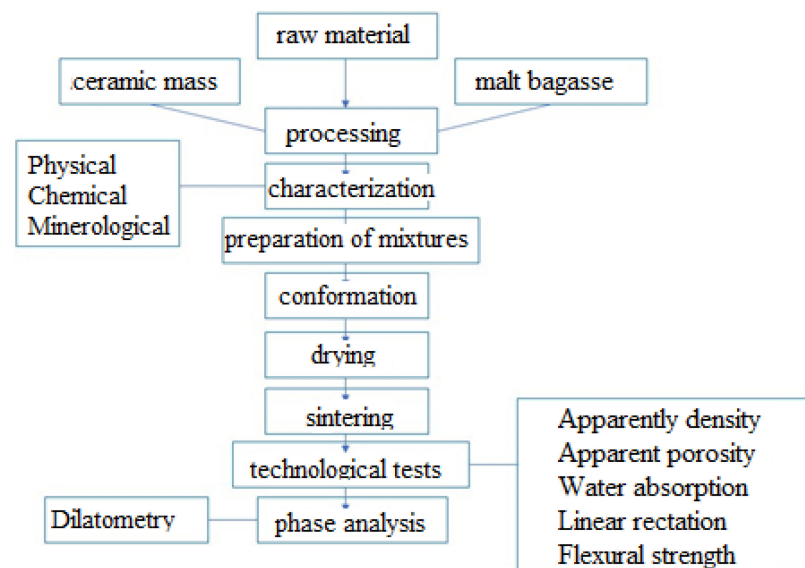


Figure 2. Experimental schedule flowchart.

2.1.1. Characterization of Raw Materials

The raw materials, including gray clay, carolinho clay, sand, and malt bagasse, underwent characterization based on their mineralogical, chemical, and physical properties. The mineralogical analysis involved the qualitative identification of crystalline phases using an X-ray diffraction (XRD) technique. The chemical composition of the materials was determined by X-ray fluorescence (XRF) analysis. Additionally, the particle size distribution was assessed through both sieving and sedimentation methods.

2.1.2. Mineralogical Analysis

- X-ray Diffraction (XRD):

The SHIMADZU brand equipment available in the Laboratory of Advanced Materials (LAMAV—UENF), was used to identify the crystalline phases in both the raw material samples and the fired ceramic pieces. The X-ray diffraction (XRD) test was conducted, wherein a beam of X-rays was directed towards a crystal, resulting in an interaction with the atoms of the sample, leading to a diffraction phenomenon. The test parameters included a 2θ range of 8° to 90° , with a step of 0.02° and a 5-s exposure time per step.

2.1.3. Chemical Analysis

- X-ray Fluorescence (XRF):

The SHIMADZU EDX700 equipment was employed to conduct a qualitative analysis of the chemical composition of the red clay and malt bagasse samples.

2.1.4. Loss to Fire

The loss on fire (LF) is typically expressed as a percentage and was obtained from the mass of the test specimens after drying and burning, according to the study by Dutra and Pontes [22]. This mass difference is attributed to the volatilization of compounds, including carbonates and organic matter, during the burning process. Thus, the loss on fire of the material can be calculated according to Equation (1):

$$LF = \frac{Ms - Mc}{Ms} \times 100 \quad (1)$$

where LF = loss on fire (%); Ms = mass of sample dried at 110°C (g); Mc = mass of the sample calcined at 1000°C for 1 h (g).

2.1.5. Elementary Analysis

- Determination of the percentage of ash:

The ash content of the samples was determined following the methodology recommended by the D1762-84 standard [23]. In crucibles previously calcined at 750 ± 25 °C for 2 h, approximately 1 g of the sample was measured and placed in a muffle at 750 °C. To prevent ignition and mass loss, the muffle was gradually heated until it reached the analysis temperature. After a period of 6 h, the samples were removed from the muffle and transferred to a desiccator until they reached room temperature. The final mass of the ash was measured, and the ash content was determined using Equation (2).

$$TC(\%) = \frac{Mc - Mcad}{Ma} \quad (2)$$

where TC = ash content (%); Mc = mass of the crucible containing the ashes (g); $Mcad$ = mass of the empty crucible (g); and Ma = sample mass (g).

- Determination of the Percentage of Sulfur:

The sulfur (S) content in the samples was determined using the energy dispersive spectroscopy (EDX) technique. The analysis was carried out using SHIMADZU equipment, specifically the model EDX-720/800HS. The equipment was equipped with a rhodium X-ray generator tube, a silicon detector, a 10 mm collimator, and a liquid nitrogen cooling system. The scanning range for the analysis varied between Na-Sc (15 kV) and Ti-U (50 kV) atoms, covering elements with atomic numbers 11–92, with a total analysis time of 100 s.

- Determination of Carbon, Hydrogen, Nitrogen, and Oxygen Content:

The carbon (C), hydrogen (H), and nitrogen (N) contents in the samples were determined using LECO CHN628 equipment. The results were processed using CHN628 software, version 1.30. The equipment was operated with helium (99.95%) and oxygen (99.99%) as carrier gases. The oven temperature was set to 950 °C, with an afterburner temperature of 850 °C. The equipment was calibrated with a standard of ethylenediaminetetraacetic acid (EDTA) with known percentages of C, H, and N (41.0% C, 5.5% H, and 9.5% N), using a mass interval between 10 and 200 mg. For analysis of the samples, 50 mg of the sample was used, supported on tin foil.

The oxygen (O) content was subsequently calculated using Equation (3), considering the sulfur and ash content.

$$O(\%) = 100(\%) - (C\% - H\% - N\% - S\% - TC\%) \quad (3)$$

where O = oxygen (%); C = carbon (%); H = hydrogen (%); N = nitrogen (%); S = sulfur (%); and TC = ash content (%).

2.1.6. Physical Analysis

- Granulometric Analysis:

The particle size distribution of the raw materials was determined using both the sieving and sedimentation methods, following the guidelines specified in NBR 7181 [20]. Through this analysis, the granulometric curve of the raw materials was used.

- Consistency Limits (Atterberg):

The plasticity of the formulations was evaluated following the procedures outlined in NBR 6459 [24] and NBR 7180 [21]. The consistency limits, also known as the Atterberg limits, include the liquidity limit (LL), the limit of plasticity (LP), and the plasticity index (PI). Thus, with the difference between the liquidity and plasticity limits, the plasticity index was determined using Equation (4).

$$PI = LL - LP \quad (4)$$

where *PI* is the plasticity index; *LL* is the liquidity limit; and *LP* is the plasticity limit.

- Linear Dilatometry:

The dilatometry test was carried out on ceramic pieces with and without malt residue using NETZSCH equipment, model DIL 402 PC, to verify the variations in dimensions and properties of the phases present in ceramic pieces with and without the addition of malt residue, subjected to a controlled temperature program, and measured as a function of time.

2.2. Mixture Preparation

Five mixtures were formulated (Table 1), incorporating different percentages of malt bagasse residue to replace the clay mass, namely 0 (reference), 2.5, 5, 10, and 15%, by mass.

Table 1. Composition of mixtures (% by mass).

Treatment (%)	Ceramic Mass (%)	Malt Bagasse (%)
0.0	100.0	0.0
2.5	97.5	2.5
5.0	95.0	5.0
10.0	90.0	10.0
15.0	85.0	15.0

Sixty grams of material (clays + sand + malt bagasse) were separated for each formulation and then homogenized in a ball mixer for 30 min. After homogenizing the mixtures, 8% of water was added in relation to the weight of each one (249.6 g) for the hydration process called “dry medium”, with the aid of a sprayer. Subsequently, they were packed in closed plastic bags to be sent to the mold to be pressed.

2.3. Conformation of the Test Specimens

From the preparation of the 5 mixtures, specimens (CPs) were molded in a rectangular shape (Figure 3) using a press with a pressure of 35 MPa and dimensions of approximately 115 × 25 × 12 mm via the pressing process. Thus, 275 CPs were made, 13 for each composition. The CPs were subjected to 4 different sintering (burning) temperatures, namely 750, 850, 950, and 1050 °C.

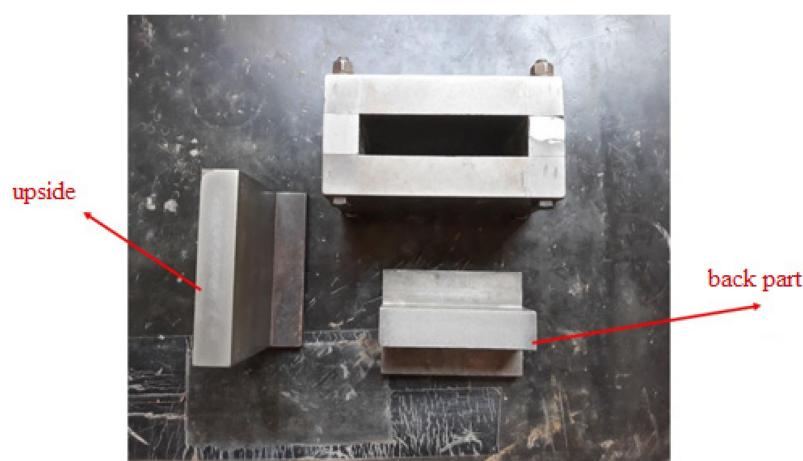


Figure 3. Mold used to form the CPs (source: author’s personal collection).

2.4. Evaluation of the L Properties of Ceramics

2.4.1. Apparent Density

The apparent density of the dry pieces was determined according to NBR ISO 10545-3 [25]. The length, width, and thickness were measured using a MITUTOYO digital caliper with a resolution of 0.01 mm, and the dry mass of the pieces was weighed using a SHIMADZU scale,

model S3000, with a precision of 0.01 g, according to NBR ISO 10545-3 [25]. Thus, the dry bulk density was calculated using Equation (5).

$$\rho_{ap} = \frac{m}{v} \quad (5)$$

where ρ_{ap} = apparent density of dry specimens (g/cm³); m = dry mass before firing (g); and v = volume of dry parts (cm³).

2.4.2. Apparent Porosity

The apparent porosity of the specimens was determined according to NBR ISO 10545-3 [25], using a SHIMADZU scale, model S3000, with a precision of 0.01 g, and calculated using Equation (6).

$$PA = \frac{Msat - Ms}{Msat - Mi} \times 100 \quad (6)$$

where PA = apparent porosity (%); $Msat$ = saturated mass (g); Ms = dry mass after firing (g); and Mi = mass of the specimen immersed in water (g).

2.4.3. Water Absorption

Water absorption was evaluated according to the ASTM C373-18 standard [26] and calculated according to Equation (7).

$$AA(\%) = \frac{Mu - Ms}{Ms} \times 100 \quad (7)$$

where AA = water absorption (%); Mu = mass (g) of the burned and wet specimen; and Ms = mass (g) of the burnt and dry specimen.

2.4.4. Linear Shrinkage

Linear shrinkage was determined to verify the dimensional variation of the samples that underwent the burning process based on NBR ISO 10545-2 [27]. Thus, the pieces were measured using a MITUTOYO digital caliper with a resolution of 0.01 mm, and linear shrinkage was calculated using Equation (8).

$$R_{Lq}(\%) = \frac{Ls - Lq}{Ls} \times 100 \quad (8)$$

where R_{Lq} = linear shrinkage; Ls = length of the pieces after drying (mm); and Lq = length of the parts after firing (mm).

2.4.5. Bending Tensile Tension

The three-point bending stress (σ) was determined using the ASTM C674-77 standard [28] and calculated using Equation (9).

$$(\sigma) = \frac{3PL}{2bd^2} \quad (9)$$

where (σ) = bending failure stress (MPa); P = load applied to the part at the moment of failure (N); L = distance between the supporting cleavers (mm); b = width of the ceramic piece (mm); and d = thickness of the specimen (mm).

2.5. Microstructural Characterization of the Specimens

The specimens from the optimal sintering temperature were subjected to morphological characterization using optical microscopy (OM) with a MOTIC Agar-Scientific microscope. The temperature of 950 °C was selected because at this temperature there is a better balance of properties, in addition to it being a commonly used sintering temperature. The samples were carefully cut and sanded to ensure a flat surface for analysis.

XRD analysis was performed using a benchtop Proto AXRD diffractometer equipped with a Cu-K α radiation source ($\lambda = 0.1541$). The instrument operated at 30 kV and 20 mA, with a platinum and nickel rotating sample filter. The goniometer radius was set to 143 mm. XRD experiments were recorded with a divergence slit of 5 mm, 2θ angle from 5° to 70° , step size of 0.02° , step multiplier of 1, and time/step of 2.5 s. In these analyses, the compositions of 10 and 15% of incorporation were not considered, because in these percentages the matrix did not present adequate behavior.

3. Statistical Analysis

For the statistical analysis, analysis of variance (ANOVA) was used to verify the existence of significant differences among the obtained results. The statistical differences were confirmed by means of the mean comparison test, using Tukey's method ($p < 0.05$).

To process the statistical data, the software Sisvar v. 5.8 [29] was used. A completely randomized design (DIC) was used since there was no separation into blocks. As for the repetitions, 13 were used for each treatment (0, 2.5, 5.0, 10, and 15%). As for interactions, temperatures, mixtures, and the breakdown between temperatures and mixtures were evaluated. Google Colab was utilized, employing the Python programming language.

4. Results and Discussion

4.1. Mineralogical Analysis

Figure 4 shows the results of the mineralogical analysis conducted on the ceramic mass used in the study. The predominant peaks observed in the ceramic mass were kaolinite (K) and quartz (Q), along with minor traces of muscovite (Mm) and gibbsite (G). Kaolinite has a tendency to form resistant phases since the transformations undergone by this mineral at high temperatures characterize a more resistant ceramic. However, the presence of quartz is essential for controlling shrinkage after firing since the material remains inert after firing when it is exposed to high temperatures; however, it also tends to decrease mechanical resistance, as demonstrated in a study by Delaqua et al. [30].

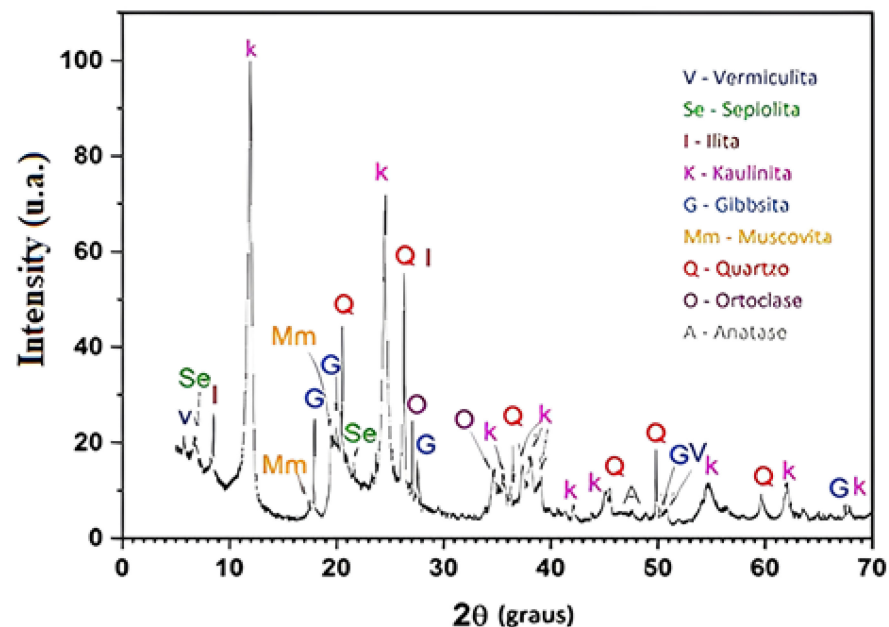


Figure 4. X-ray diffractograms of the ceramic mixture used.

4.2. Chemical Analysis

XRF and PF analyses were performed on the raw materials used (clays and sand), as shown in Table 2.

Table 2. Chemical composition of raw materials used in XRF.

Composition	SiO ₂	Al ₂ O ₃	Fe ₂ O ₃	TiO ₂	K ₂ O	MgO	Na ₂ O	CaO	Others	PF
Gray clay	47.04	32.56	3.48	1.29	1.01	0.55	0.34	0.24	0.10	13.39
Carolinho	49.34	30.71	3.66	1.21	0.99	0.61	0.24	0.22	0.11	12.91
Sand	81.10	11.90	1.20	0.47	1.50	0.62	0.84	0.51	0.16	1.70

Through XRF analysis, higher levels of silica (SiO₂) and alumina (Al₂O₃) were identified. The elevated SiO₂ content is associated with the silicates present (clay minerals, mica, feldspars) and free silica (quartz) [31], primarily found in the sand component. The high content of alumina (Al₂O₃) and the low content of flux oxides present (K, Na) in the clays (ball clay) can be associated with the low formation of eutectics in the material, which attributes refractory characteristics to the clay [32]. Due to the presence of both compounds, the clays used were predominantly kaolinitic, as confirmed by Klitzke [33] and Vieira and Pinheiro [34].

As for the sand component, which was predominantly made up of SiO₂, the presence of alkaline and alkaline earth oxides can be observed, which are characterized as fluxes when subjected to high temperatures [35]. In addition, for clays, a high fire loss can be verified, which contributes to an increase in the porosity and shrinkage of ceramics, thus interfering with the mechanical properties of the pieces [34]. The low content of iron III oxide (Fe₂O₃), an element responsible for the coloration of clays, justifies the gray color, considering that the lower this content, the clearer and less reddish the clay is after firing [36].

4.3. Elementary Analysis

The results of the elemental analysis of the malt residue are shown in Table 3. The malt bagasse residue was characterized by organic matter due to the presence of a high carbon content (45.52%), as well as high oxygen (O) and hydrogen (H) contents, as stated in the study by Aqsha et al. [37] and Machado et al. [38]. Small variations usually occur according to the period of harvest, malting, and other additions [39]. The C and H content contribute to the energy density characteristics of the material, which are directly linked to the calorific value of the substance. As for the presence of nitrogen (N) and sulfur (S), the low compositions can be highlighted, which is beneficial due to the low emissions to the environment. In addition, the volatile matter content associated with the low ash content is favorable for thermochemical conversion [38].

Table 3. Elemental composition of malt residue (%).

Composition (%)	C	H	N	S	O	Ashes
Malt	45.52	7.30	4.52	0.23	39.76	2.67

4.4. Granulometry of Raw Materials

Figure 5 illustrates the granulometry of the raw materials (carolinho and gray clays—ball clay and sand) used in the ceramic mass preparation.

The different size ranges are associated with the clay, silt, and fine sand and coarse sand fractions, according to the granulometric classification according to NBR 7181 [20]. The clay fraction (ball clay—gray clay particles and carolinho) was associated with particles with spherical diameters smaller than 2 µm, which gives the raw materials plasticity when mixed with water, and was associated with clay minerals [40]. This fraction is also related to the granulometry of kaolinite, which is a clay mineral found in kaolin and is responsible for plasticity in clays, which is a typical characteristic of clays from Campos dos Goytacazes, RJ [34]. However, the sand presented particles with dimensions from 2 to 0.06 mm, mainly composed of quartz grains, which was confirmed by the XRF analysis performed (Table 2).

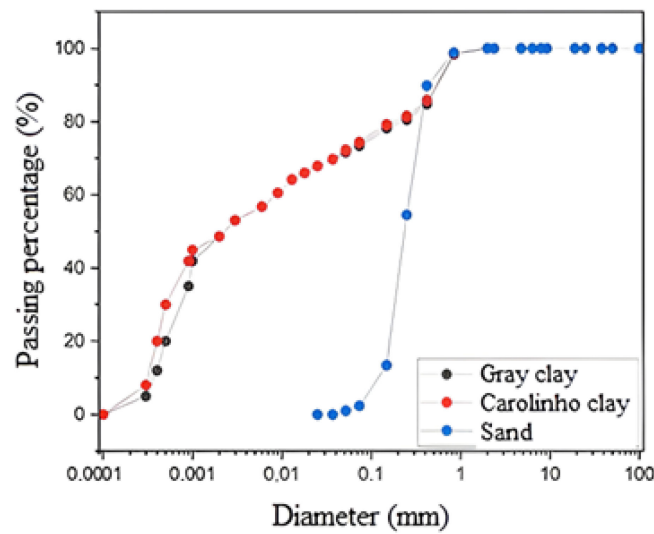


Figure 5. Granulometry of the raw materials used in the ceramic mass.

Thus, the presence of sand (quartz) is important to adjust the plasticity/workability of the clay and to reduce the drying and firing shrinkage of ceramics, as confirmed by Vieira and Pinheiro [34]. However, the granulometric fractions meet their use in ceramics ($30\% \leq \text{clay fraction} \leq 70\%$), as stated by Pedroti et al. [41].

4.5. Consistency Limits (Atterberg)

Although this study did not involve the conventional extrusion process by pressing, it is important to discuss the Atterberg limits, considering the potential industrial scale applications after the study. Figure 6 presents the results consistency limits of the clayey mass used. According to the prognosis of extrusion by the pressing of the ceramic pieces in relation to the malt bagasse content using the Atterberg limits (Figure 6), it can be observed that the samples containing 0 (reference), 2.5, and 5% malt bagasse fall within the acceptable extrusion demarcated area. However, the samples manufactured with 10 and 15% malt bagasse lie outside this range. This observation can be attributed to the fact that the limit of plasticity (LP) represents the minimum amount of water required for the clay to reach the necessary consistency for plastic formation [18]. Consequently, the water added to the ceramic mass acts to fill the pores between the particles and facilitate the shaping of the pieces, as described in Silva [42].

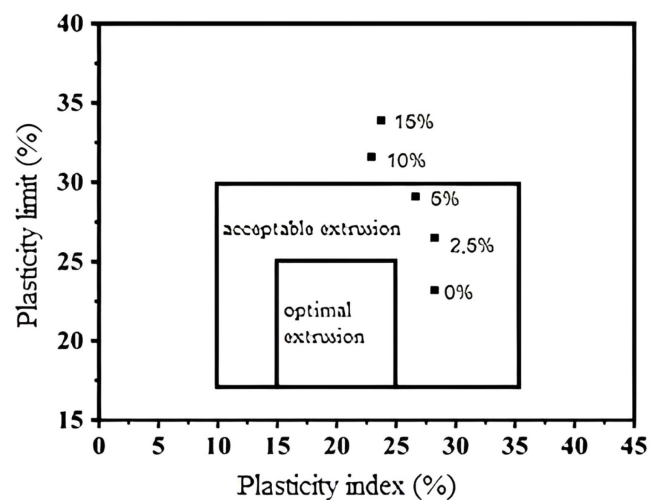


Figure 6. Prediction of press extrusion through Atterberg limits.

The pieces manufactured with 0, 2.5, and 5% malt bagasse exhibited a plasticity index (IP) between 25% and 30% and a limit of plasticity (LP) between 20% and 30%, which falls within the acceptable range for conformation according to Vieira et al. [43]. The authors suggested that LP values between 22% and 24% can be considered acceptable, with a minimum IP of 10%. However, the pieces containing 10 and 15% residue displayed a high LP, exceeding 30%, making them unviable for conformation. The higher percentage of malt residue in ceramics can be associated with this lack of feasibility. Malt residue possesses a hydrophilic characteristic, meaning it has a greater tendency to absorb water [12]. When combined with the mineralogical characteristics and high plasticity of the clay used, it necessitates the addition of a larger amount of water during the conformation stage. This increased water content increases the likelihood of cracks and deformations due to greater retraction of the pieces [43].

4.6. Technological Properties of Ceramics

4.6.1. Dilatometry

As depicted in Figure 7, the curves corresponding to the ceramics produced with 0% (reference) and 15% malt bagasse were examined to assess the transformation of phases during the sintering stages, as previously demonstrated by Ribeiro et al. [44].

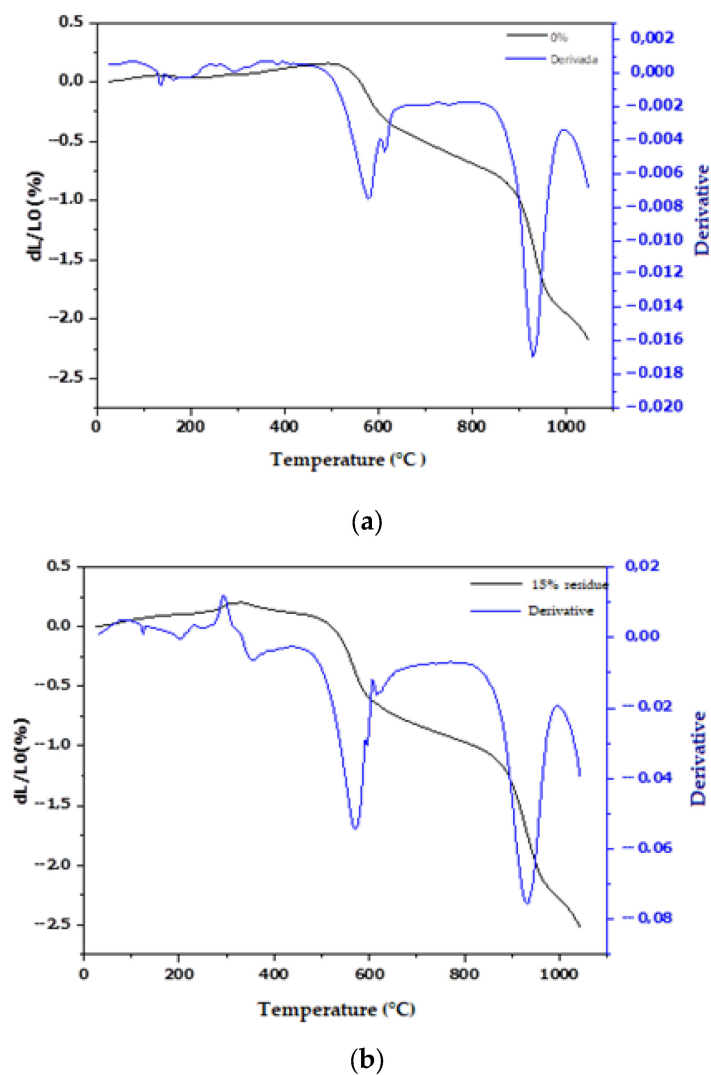


Figure 7. Dilatometry of ceramic pieces: (a) 0%; (b) 15% malt bagasse.

Both samples exhibited a decrease in the curve around 550 °C, as indicated by the exothermic peaks. Close to 550 °C, the quartz transforms, accompanied by an expansion of the crystalline structure and of gases remaining from the combustion of the organic residue [30]. However, the peak observed for the reference sample (0% incorporation) was lower than of the 15% sample, which can be attributed to the shrinkage that occurred within the material [30]. Larger quantities of the liquid phase typically result in greater shrinkage [44].

During the firing process, the ceramic pieces can experience various heating-related defects. These defects occur at temperatures above 100 °C, when hygroscopic water begins. Above 200 °C, colloidal water, which is water-bound to the clay particles and remains even after drying, is eliminated [45,46]. At temperatures exceeding 400 °C, the organic substances present in the pieces start to burn, and additional reactions take place, such as the dehydroxylation of kaolinite, the transformation of quartz, and the release of water (combined in kaolinite) from the clay's constitution [45]. As the temperature reaches 700 °C, the chemical reactions occur between silica and alumina and fluxing elements, resulting in the formation of silica–aluminous complexes. These complexes contribute to the hardness, strength, and stability of the ceramics [45,46]. At 900 °C, the combustion process of the organic material takes place, which is confirmed by the high loss of ignition in the XRF analysis shown in Table 2 and the elemental analysis in Table 3. The combustion occurs in two stages: a homogeneous stage involving the combustion of volatile compounds and a heterogeneous stage involving waste combustion [30,47] in which the carbonates decompose, releasing CO₂. Above 1000 °C, the silico–aluminous compounds, which are in vitreous form, begin to soften, causing the ceramic body to undergo drainage and deformation in the final phase of firing [45].

4.6.2. Apparent Density

Table 4 presents the dry bulk density of the ceramics. In terms of apparent dry density, significant differences were observed among the values obtained for the waste incorporation treatments. However, no significant difference was found for the sintering temperature, except for the case involving 2.5% malt, as illustrated in Figure 8.

Table 4. Apparent dry density of ceramics.

Malt Bagasse (%)	Apparent Dry Density (g.cm ⁻³) *			
	Sintering Temperature (°C)			
	750	850	950	1050
0.0	1.83 aD	1.83 aC	1.83 aD	1.85 aD
2.5	1.83 abD	1.81 aC	1.84 bD	1.83 abD
5.0	1.80 aC	1.80 aC	1.79 aC	1.79 aC
10.0	1.74 aB	1.73 aB	1.72 aB	1.71 aB
15.0	1.59 aA	1.59 aA	1.60 aA	1.61 aA

* Means followed by the same letter, lowercase in the row and uppercase in the column, do not differ by Tukey's test at the 5% probability level ($p < 0.05$).

However, a decreasing trend in density was observed as the levels of biomass residue incorporated into the ceramics increased, which is consistent with the findings by Cotes-Palomino et al. [48]. This lower density characteristic is intrinsic to lignocellulosic biomass [38] and is attributed to its organic composition and biodegradability, particularly when exposed to high temperatures. This is evident from the significant differences in the treatments in relation to temperature. Nevertheless, this mass reduction in mass does not adversely affect the performance of the ceramic material and can even be considered advantageous, as ceramic materials are commonly used as sealing blocks or tiles [17,30].

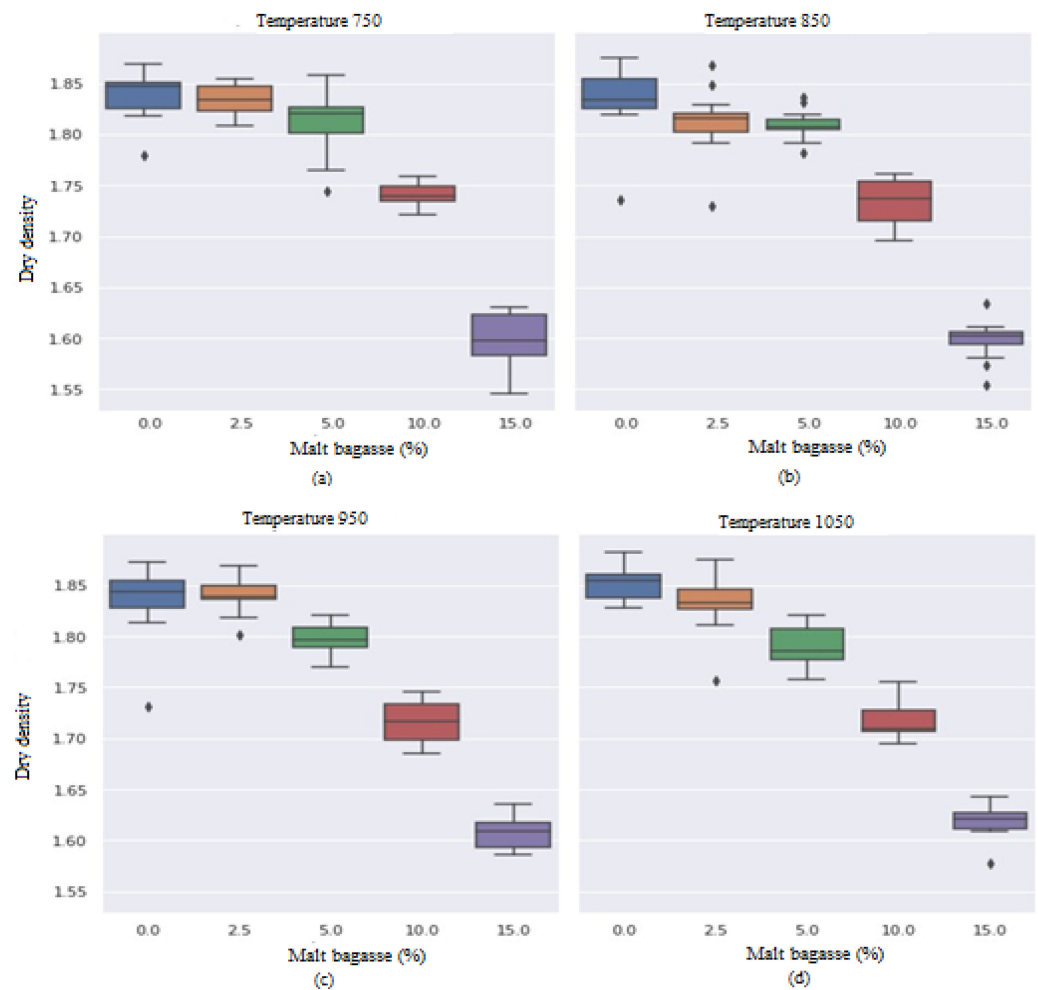


Figure 8. Behavior of ceramic pieces in terms of dry density: (a) 750 °C; (b) 850 °C; (c) 950 °C; (d) 1050 °C.

4.6.3. Apparent Porosity

Table 5 and Figure 9 display the apparent porosity results for the manufactured ceramics.

Table 5. Apparent porosity (%) of ceramics.

Malt Bagasse (%)	Apparent Porosity (%) *			
	Sintering Temperature (°C)			
	750	850	950	1050
0.0	27.57 dA	26.99 cA	26.56 bA	25.20 aA
2.5	27.87 dA	27.35 cB	26.75 bA	25.33 aA
5.0	28.27 dB	27.76 cC	27.20 bB	25.95 aB
10.0	29.67 dC	29.24 cD	28.65 bC	27.95 aC
15.0	31.18 cD	31.40 cE	30.68 bD	30.31 aD

* Means followed by the same letter, lowercase in the row and uppercase in the column, do not differ by Tukey's test at the 5% probability level ($p < 0.05$).

There was a significant difference observed between the treatments, both in terms of residue incorporation and sintering temperature. With the increase in malt bagasse, there was an increase in porosity in relation to the reference sample (0% incorporation). During the sintering process, the samples with malt bagasse exhibited a higher propensity for the formation pores in the ceramic, which is also associated with a loss of mass that consequently causes more porosity, as confirmed by Russ et al. [49].

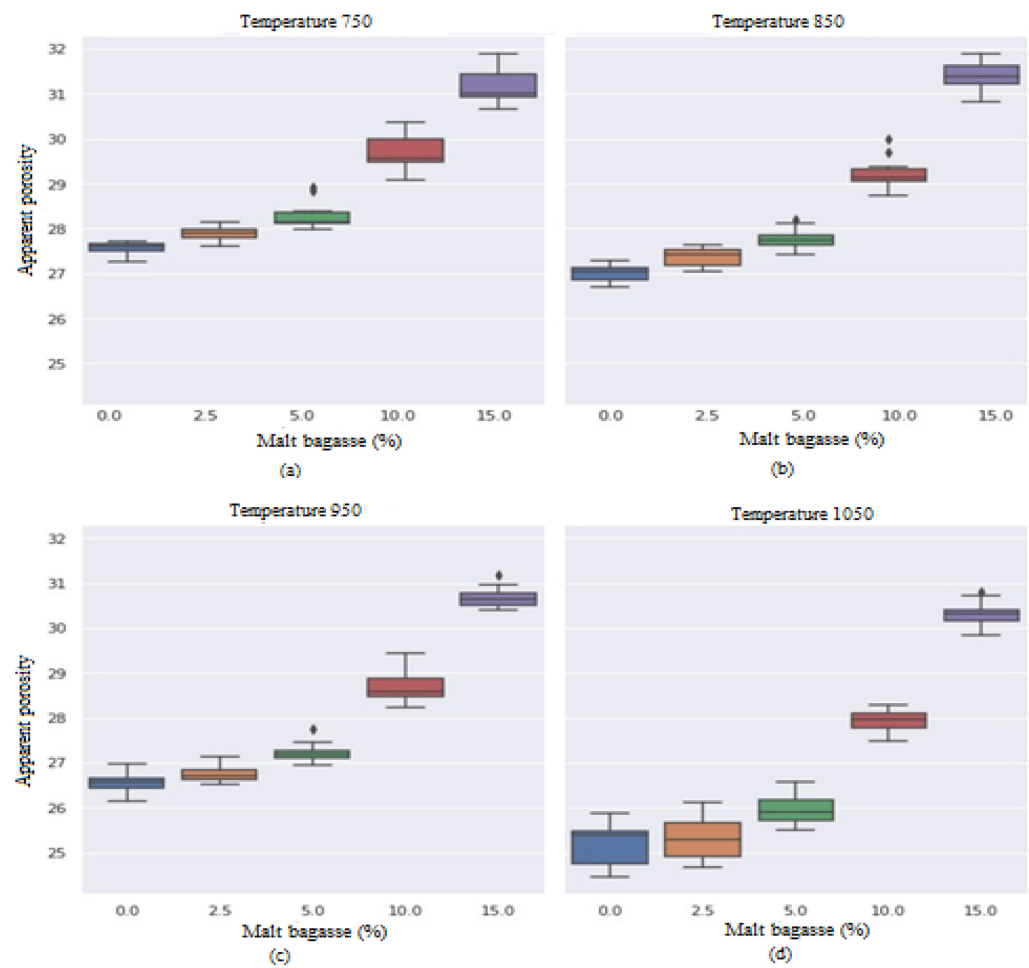


Figure 9. Behavior of ceramic pieces regarding apparent porosity: (a) 750 °C; (b) 850 °C; (c) 950 °C; (d) 1050 °C.

4.6.4. Water Absorption

Regarding water absorption, the results are presented in Table 6.

Table 6. Water absorption (%) of ceramics.

Malt Bagasse (%)	Water Absorption (%) *			
	Sintering Temperature (°C)			
	750	850	950	1050
0.0	19.03 bA	19.15 bA	19.01 bA	16.05 aA
2.5	19.00 bA	19.22 bA	18.67 bA	15.57 aA
5.0	18.72 bA	19.00 bA	18.67 bA	15.93 aA
10.0	22.52 bB	23.07 bB	22.60 bB	20.99 aB
15.0	28.54 abC	29.07 bcC	29.29 cC	28.29 aC

* Means followed by the same letter, lowercase in the row and uppercase in the column, do not differ by Tukey's test at the 5% probability level ($p < 0.05$).

The test specimens manufactured with varying proportions of malt bagasse residue exhibited a significant difference between the percentages of malt bagasse incorporation and the sintering temperatures, as depicted in Figure 10. With an increase in the amount of residue incorporated, there was a corresponding increase in water absorption. This can be attributed to the hydrophilic characteristics [49] and the combustion of organic compounds present in biomass [30], which also contributes to the elevation of porosity. Consequently, higher porosity results in greater water absorption [50]. However, at a sintering temperature

of 1050 °C, there was a reduction in porosity, which may be associated with the enhanced formation of the liquid phase, a primary mechanism in ceramic sintering [30].

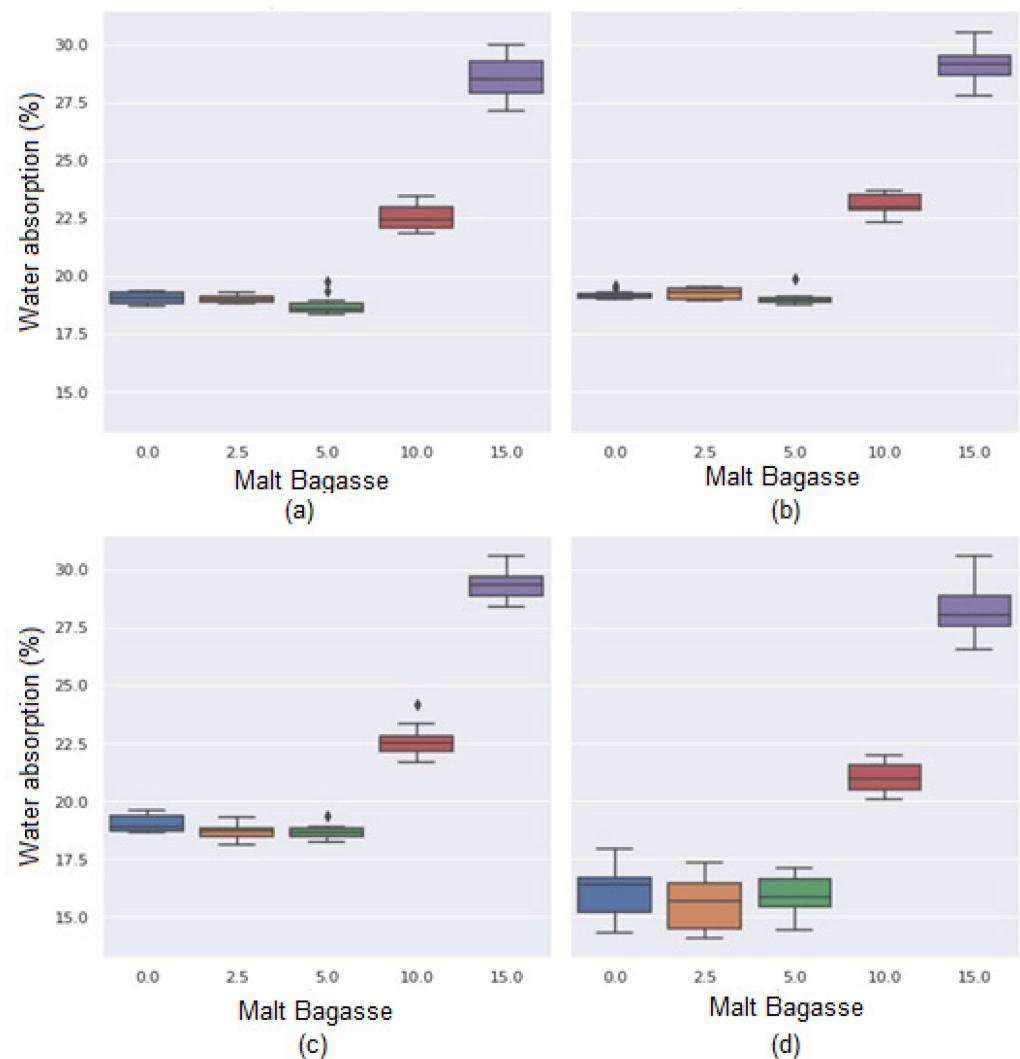


Figure 10. Behavior of ceramic pieces in terms water absorption: (a) 750 °C; (b) 850 °C; (c) 950 °C; (d) 1050 °C.

The maximum allowable water absorption value according to technical standards is up to 25% for ceramic sealing blocks [51] and up to 20% for tiles [52]. Therefore, for treatments of up to 5%, the incorporation of malt bagasse residue can be recommended for ceramic blocks in terms of water absorption, regardless of the sintering at all temperatures studied. In the case of tiles, only the ceramic mass containing 2.5% fired at 1050 °C was found to be viable for application, taking into consideration the other evaluated properties as well.

4.6.5. Linear Shrinkage

Table 7 displays the results of linear shrinkage for the manufactured ceramics.

Table 7. Linear shrinkage of ceramics.

Malt Bagasse (%)	Linear Shrinkage *			
	Sintering Temperature (°C)			
	750	850	950	1050
0.0	0.88 aBC	1.24 bA	2.00 cB	3.31 dC
2.5	0.71 aAB	1.26 bC	1.92 cB	3.32 dC
5.0	0.62 aAB	0.95 bAB	1.46 cA	2.73 dB
10.0	0.53 aA	0.88 bA	1.21 cA	1.94 dA
15.0	1.10 aC	1.20 aBC	1.74 bB	2.64 cB

* Means followed by the same letter, lowercase in the row and uppercase in the column, do not differ by Tukey's test at the 5% probability level ($p < 0.05$).

There was a significant difference in the linear shrinkage of the ceramic pieces as they increased with the rise in firing temperature for all treatments. This can be attributed to the improved arrangement of particles through the formation of a liquid phase, which facilitates their approximation and subsequently their shrinkage [30]. Notably, there was a considerable increase in shrinkage for all ceramics fired at 1050 °C, indicating transformations in the sintering stage that result in the formation of more resistant compounds. During this sintering phase, there is an increase in the amount of the liquid phase present in the material due to the amount of alkaline and alkaline earth compounds, densifying the specimens more and consequently causing greater linear shrinkage [53]. The maximum recommended shrinkage for ceramic firing is 2% [30]; this was exceeded only at 1050 °C for all treatments studied in this case.

4.6.6. Fracture Strength on the Bending of the Test Specimens

The analysis of flexural strength in the specimens produced with different contents of malt bagasse residue revealed a significant difference between the percentages of malt bagasse incorporation as well as between the sintering temperatures (Table 8). Regarding the sintering temperatures, all ceramic masses exhibited an increase in flexural rupture stress as the firing temperature increased compared to the reference pieces (0% malt bagasse). Furthermore, for all treatments, there was a significant increase in the tensile strength of the sintered mixtures, from 750 to 850 °C. This can be attributed to the greater loss of adsorbed water and the reduction of initial mass during the firing process. At 850 °C, the tensile strengths of all treatments remained relatively stable in this regard.

Table 8. Mean fracture strength (MPa) of the samples in relation to the sintering temperature (°C) and the incorporation of malt bagasse residue (%).

Malt Bagasse (%)	Fracture Strength to Bending (MPa) *			
	Sintering Temperature (°C)			
	750	850	950	1050
0.0	3.45 aD	4.45 bC	4.62 bD	5.17 cD
2.5	3.15 aC	4.16 bC	4.21 bC	4.28 bC
5.0	2.00 aB	2.42 bB	2.49 bB	2.74 cB
10.0	0.85 aA	0.98 abA	1.09 bcA	1.23 cA
15.0	0.85 aA	0.98 abA	1.09 bcA	1.23 cA

* Means followed by the same letter, lowercase in the row and uppercase in the column, do not differ by Tukey's test at the 5% probability level ($p < 0.05$).

In relation to the incorporation of malt bagasse, there is a direct correlation between the amount of residue incorporated and the decrease in bending stress of the ceramic pieces. This effect is particularly noticeable at a 15% residue incorporation, where the lowest bending stress is observed. This behavior can be attributed to the lignocellulosic characteristics of the malt residue, which undergoes significant degradation and becomes more fragile

at high temperatures [12]. This results in significant loss in mass, leading to a reduction in the area under applied stress and an increase in porosity compared to the reference piece (0% incorporation). Additionally, the manufactured material exhibited a reduced number of crystalline phases, which contributes to the mechanical strength of ceramic materials [33]. However, it is important to note that the recommended minimum value for ceramic masonry components is 2.0 MPa, as demonstrated by Ketov et al. [54]. Therefore, the incorporation of up to 5% malt bagasse at all studied temperatures is recommended as it allows for an acceptable level of bending stress while still benefiting from the potential advantages of incorporating the residue.

4.7. Microstructure of the Test Specimens

Figure 11 shows the result of the optical micrograph of the different compositions sintered at 950 °C.

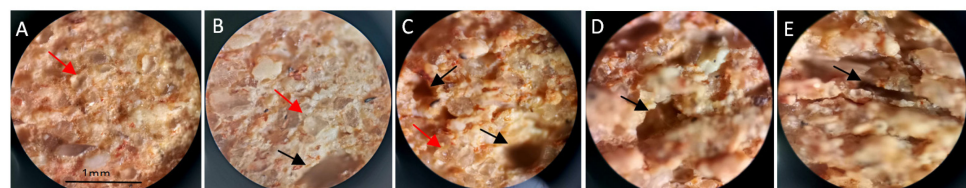


Figure 11. Optical micrograph: (A) 0%; (B) 2.5%; (C) 5.0%; (D) 10.0%; (E) 15.0%.

Figure 11 clearly demonstrates that the red arrows highlight the porosity of the material, which plays a fundamental role in properties associated with mechanical strength and water absorption. As the sintering temperature increases, there is a consequent reduction in porosity, as evidenced by previous results. The micrograph supports this finding by illustrating that the increased addition of agro-industrial residue leads to an increase in porosity, indicated by the white dots in the micrographs. The black arrows indicate quartz grains, resulting from thermal transformations within the ceramic matrix. In Figure 11E, a visible crack can be observed, possibly caused by the high concentration of the residue, leading to defects in the ceramic matrix.

Figure 12 illustrates the results of X-ray diffraction (XRD) analysis, where the compositions of 10% and 15% were excluded from the analysis due to insufficient values and the presence of excessive cracks, as identified and verified previously.

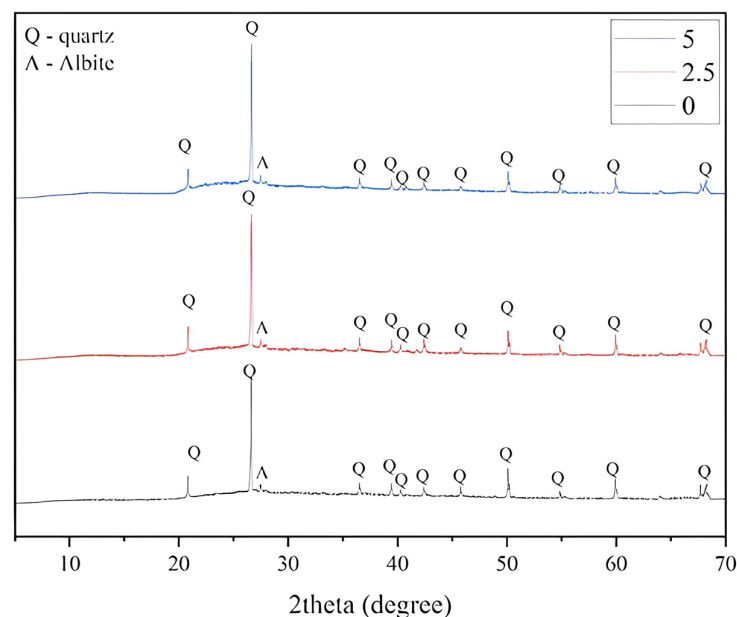


Figure 12. Results of X-ray diffraction (XRD).

The diffractograms depicted in Figure 12 demonstrate a prevalence of Quartz and Albite, minerals commonly found in ceramic materials, supporting existing literature and aligning with the micrographs presented in Figure 11 [36,45].

5. Conclusions

The ceramic mass utilized was primarily characterized by the presence of kaolinite and quartz, indicating a tendency to form a ceramic material that is more resistant and controlled in terms of shrinkage after firing. The clays used were predominantly kaolinitic and had refractory characteristics of ceramic material. The malt bagasse residue used was characterized by its organic composition, primarily consisting of high levels of carbon, oxygen, and hydrogen.

Regarding the ceramic pieces manufactured with the incorporation of malt bagasse residue, there was a reduction in density as the residue content increased. However, this reduction in mass did not negatively impact the performance of the ceramic material when incorporated up to 5%. In fact, it could even be considered advantageous since ceramic materials are commonly utilized as sealing blocks or tiles.

The samples with higher levels of malt bagasse incorporation exhibited a greater tendency towards the formation of pores in the ceramics. These pores are associated with a loss of mass, resulting in increased porosity and higher water absorption in these ceramics. However, for treatments involving up to 5% malt bagasse incorporation, it is recommended for ceramic blocks due to their water absorption characteristics, regardless of the sintering temperatures employed.

The treatments demonstrated a significant increase in the tensile strength of the sintered mixtures, from 750 to 850 °C. Above 850 °C, the tensions of all treatments remained relatively stable. Consequently, the higher the quantity of malt bagasse residue incorporated, the lower the bending stress exhibited by the components. Incorporating up to 5% malt bagasse at all investigated temperatures is advisable for masonry ceramic components.

Author Contributions: Conceptualization, J.P.d.S.C.A., D.C. and J.L.P.; methodology, J.P.d.S.C.A., D.C., C.M.F.V. and G.C.G.D.; validation, J.P.d.S.C.A., D.C., L.d.S.H. and T.R.d.S.; formal analysis, M.A., J.L.P. and C.M.H.; investigation, L.d.S.H., T.R.d.S. and J.P.d.S.C.A.; writing—original draft preparation, J.P.d.S.C.A., D.C. and C.M.F.V.; writing—review and editing, D.C., F.C.d.S., M.A., J.L.P., C.M.H., D.d.F.d.C. and A.R.G.d.A.; supervision, A.R.G.d.A.; project administration, A.R.G.d.A. and D.C. All authors have read and agreed to the published version of the manuscript.

Funding: The participation of A.R.G.A. was sponsored by FAPERJ through the research fellowships proc. no: E-26/210.150/2019, E-26/211.194/2021, E-26/211.293/2021, and E-26/201.310/2021 and by CNPq through the research fellowship PQ2 307592/2021-9.

Institutional Review Board Statement: Not applicable.

Informed Consent Statement: Not applicable.

Data Availability Statement: Not applicable.

Acknowledgments: The authors acknowledge the Brazilian governmental research agencies CAPES (Coordenação de Aperfeiçoamento de Pessoal de Nível Superior), CNPq (Conselho Nacional de Desenvolvimento Científico e Tecnológico), and FAPERJ (Fundação de Amparo à Pesquisa do Estado do Rio de Janeiro).

Conflicts of Interest: The authors declare no conflict of interest.

References

1. Azevedo, A.R.G.; Cruz, A.S.A.; Marvila, M.T.; Oliveira, L.B.D.; Monteiro, S.N.; Vieira, C.M.F.; Fediuk, R.; Timokhin, R.; Vatin, N.; Daironas, M. Natural Fibers as an Alternative to Synthetic Fibers in Reinforcement of Geopolymer Matrices: A Comparative Review. *Polymers* **2021**, *13*, 2493. [[CrossRef](#)]
2. Cheremisinoff, N.P.; Rosenfeld, P.; Davletshin, A.R. The Food and Dairy Industry. *Responsible Care* **2008**, *45*, 383–434.
3. Swart, L.J.; Petersen, A.M.; Bedzo, O.K.K.; Görgens, J.F. Techno-economic analysis of the valorization of brewers spent grains: Production of xylitol and xylo-oligosaccharides. *J. Chem. Technol. Biotechnol.* **2021**, *96*, 1632–1644. [[CrossRef](#)]

4. Mussatto, S.I.; Dragone, G.; Teixeira, J.A.; Roberto, I.C. Total reuse of brewer's spent grain in chemical and biotechnological processes for the production of added-value compounds. In Proceedings of the Bioenergy: Challenges and Opportunities—International Conference and Exhibition on Bioenergy, Guimarães, Portugal, 6–9 April 2008; Minho's University: Guimarães, Portugal, 2008.
5. Potential for Consumption of Beer in Brazil. 2014. Available online: <https://bis.sebrae.com.br/bis/conteudoPublicacao.zhtml?id=4864> (accessed on 6 October 2022).
6. Bonato, S.V.; Pacheco, D.A.J.; Caten, C.S.; Caro, C. The missing link of circularity in small breweries' value chains: Unveiling strategies for waste management and biomass valorization. *J. Clean. Prod.* **2022**, *336*, 130275. [[CrossRef](#)]
7. Silva, T.R.; Azevedo, A.R.G.; Cecchin, D.; Marvila, M.T.; Fediuk, R.; Amran, M.; Vatin, N.; Karelina, M.; Klyuev, S.; Szelag, M. Application of Plastic Wastes in Construction Materials: A Review Using the Concept of Life-Cycle Assessment in the Context of Recent Research for Future Perspectives. *Materials* **2021**, *14*, 3549. [[CrossRef](#)] [[PubMed](#)]
8. León-González, M.E.; Gómez-Mejía, E.; Rosales-Conrado, N.; Madrid-Albarrán, Y. Residual brewing yeast as a source of polyphenols: Extraction, identification and quantification by chromatographic and chemometric tools. *Food Chem.* **2018**, *267*, 246–254. [[CrossRef](#)] [[PubMed](#)]
9. Ashraf, A.; Ramamurthy, R.; Rene, E.R. Wastewater treatment and resource recovery technologies in the brewery industry: Current trends and emerging practices. *Sustain. Energy Technol. Assess.* **2021**, *47*, 101432. [[CrossRef](#)]
10. Czubaszek, A.; Wojciechowicz-Budzisz, A.; Sychaj, R.; Kawa-Rygielska, J. Baking properties of flour and nutritional value of rye bread with brewer's spent grain. *LWT-Food Sci. Technol.* **2021**, *150*, 111955. [[CrossRef](#)]
11. Codina-Torrella, I.; Rodero, L.; Almajano, M.P. Brewing By-Products as a Source of Natural Antioxidants for Food Preservation. *Antioxidants* **2021**, *10*, 1512. [[CrossRef](#)]
12. Cordeiro, L.G.; El-Aouar, Â.A.; De Araújo, C.V.B. Energetic characterization of malt bagasse by calorimetry and thermal analysis. *J. Therm. Anal. Calorim.* **2013**, *112*, 713–717. [[CrossRef](#)]
13. Ferreira, D.C.M.; Molina, G.; Pelissari, F.M. Biodegradable trays based on cassava starch blended with agroindustrial residues. *Compos. Part B* **2020**, *183*, 107682. [[CrossRef](#)]
14. Lopes, A.C.; Klosowski, A.B.; Carvalho, B.M.; Olivato, J.B. Application and characterisation of industrial brewing by products in biodegradable starch-based expanded composites. *Int. J. Food Sci. Technol.* **2022**, *57*, 5523–5531. [[CrossRef](#)]
15. Quaranta, N.; Caligaris, M.; Pelozo, G.; Unsen, M.; Cristóbal, A. The characterization of brewing waste and feasibility of its use for the production of porous ceramics. *Waste Manag. Environ. VIII* **2016**, *202*, 299–310.
16. Stefani, D.; Dahlem Júnior, M.A.; Francisquetti, E.L.; Reis, F.S.; Borsoi, C.; Hansen, B.; Catto, A.L. Influence of coupling agent on post-consumption polypropylene composites reinforced with malt bagasse fibers. *J. Compos. Mater.* **2021**, *55*, 4333–4346. [[CrossRef](#)]
17. Luiz, N.F.; Cecchin, D.; Azevedo, A.R.G.; Alexandre, J.; Silva, F.C.; Paes, A.L.C.; Pinheiro, V.D.; Do Carmo, D.F.; Ferraz, P.F.P.; Hüther, C.M.; et al. Characterization of materials used in the manufacture of ceramic tile with incorporation of ornamental rock waste. *Agron. Res.* **2020**, *18*, 904–914.
18. Silva, T.R.; Cecchin, D.; Azevedo, A.R.G.; Valadão, I.; Alexandre, J.; Silva, F.C.; Marvila, M.T.; Gunasekaran, M.; Garcia Filho, F.; Monteiro, S.N. Technological Characterization of PET—Polyethylene Terephthalate—Added Soil-Cement Bricks. *Materials* **2021**, *14*, 5035. [[CrossRef](#)]
19. Eliche-Quesada, D.; Martínez-García, C.; Martínez-Cartas, M.L.; Cotes-Palomino, M.T.; Pérez-Villarejo, L.; Cruz-Pérez, N.; Corpas-Iglesias, F.A. The use of different forms of waste in the manufacture of ceramic bricks. *Appl. Clay Sci.* **2011**, *52*, 270–276. [[CrossRef](#)]
20. *NBR 7181*; Erratum 2:2018: Soil—Particle Size Analysis. Brazilian Association of Technical Standards—ABNT: Rio de Janeiro, Brazil, 2016. (In Portuguese)
21. *NBR 7180*; Soil—Determination of Plasticity Limit. Brazilian Association of Technical Standards—ABNT: Rio de Janeiro, Brazil, 2016. (In Portuguese)
22. Dutra, R.P.S.; Pontes, L.R.A. Obtaining and analysis of porous ceramic with the incorporation of organic products to the ceramic body. *Cerâmica* **2002**, *48*, 223–230. [[CrossRef](#)]
23. *D1762-84*; Standard Test Method for Chemical Analysis of Wood Charcoal. American Society for Testing and Materials—ASTM: New York, NY, USA, 2021.
24. *NBR 6459*; Erratum 1:2017: Soil—Determination of the Liquidity Limit. Brazilian Association of Technical Standards—ABNT: Rio de Janeiro, Brazil, 2016. (In Portuguese)
25. *NBR ISO 10545-3*; Ceramic Tiles—Part 3: Determination of Water Absorption, Apparent Porosity, Apparent Relative Density and Apparent Density—Corrected in 2020. Brazilian Association of Technical Standards—ABNT: Rio de Janeiro, Brazil, 2018. (In Portuguese)
26. *C373-18*; Standard Test Methods for Determination of Water Absorption and Associated Properties by Vacuum Method for Pressed Ceramic Tiles and Glass Tiles and Boil Method for Extruded Ceramic Tiles and Non-tile Fired Ceramic Whiteware Products. American Society for Testing and Materials—ASTM: New York, NY, USA, 2018.
27. *NBR ISO 10545-2*; Ceramic Tiles—Part 2: Determination of dimensions and Surface Quality—Corrected in 2020. Brazilian Association of Technical Standards—ABNT: Rio de Janeiro, Brazil, 2018. (In Portuguese)
28. *C674-77*; Flexural Properties of Ceramic Whiteware Materials. American Society for Testing and Materials—ASTM: New York, NY, USA, 1977.
29. Ferreira, D.F. Sisvar: A Guide for its bootstrap procedures in multiple comparisons. *Ciênc. Agrotec.* **2014**, *38*, 109–112. [[CrossRef](#)]

30. Delaqua, G.C.G.; Marvila, M.T.; Souza, D.; Rodriguez, R.S.J.; Colorado, H.A.; Vieira, C.M.F. Evaluation of the application of macrophyte biomass *Salvinia auriculata* Aublet in red ceramics. *J. Environ. Manag.* **2020**, *275*, 111253. [[CrossRef](#)]
31. Avelino, K.A.R. Study of the Potential of Incorporating Granite Waste and Coffee Husk Burning into Red Ceramics. Master's Thesis, Graduate Program in Materials Science and Engineering, Federal University of Rio Grande do Norte, Natal, Brazil, 2013. (In Portuguese).
32. Vieira, C.M.F.; Monteiro, S.N. Influence of the firing temperature on the microstructure of clays from Campos dos Goytacazes-RJ. *Cerâmica* **2003**, *49*, 6–10. [[CrossRef](#)]
33. Klitzke, W. Use of Forest Biomass Ash as a Porogenic Agent in Ceramic Material. Ph.D. Thesis, Department of Agricultural Sciences, Graduate Program in Forestry Engineering, Federal University of Paraná, Curitiba, Paraná, 2020. (In Portuguese).
34. Vieira, C.M.F.; Pinheiro, R.M. Evaluation of kaolinitic clays from Campos dos Goytacazes used for red ceramic fabrication. *Cerâmica* **2011**, *57*, 319–323. [[CrossRef](#)]
35. Vieira, C.M.F.; Monteiro, S.N. Clayey ceramic incorporated with oily waste from the petroleum industry. *Matéria* **2006**, *11*, 217–222. (In Portuguese)
36. Vieira, C.M.F.; Sánchez, R.; Monteiro, S.N. Characteristics of clays and properties of building ceramics in the state of Rio de Janeiro, Brazil. *Constr. Build. Mater.* **2008**, *22*, 781–787. [[CrossRef](#)]
37. Aqsha, A.; Tijani, M.M.; Moghtaderi, B.; Mahinpey, N. Catalytic pyrolysis of straw biomasses (wheat, flax, oat and barley) and the comparison of their product yields. *J. Anal. Appl. Pyrolysis* **2017**, *125*, 201–208. [[CrossRef](#)]
38. Machado, L.M.M.; Lütke, S.F.; Perondi, D.; Godinho, M.; Oliveira, M.L.S.; Collazzo, G.C.; Dotto, G.L. Simultaneous production of mesoporous biochar and palmitic acid by pyrolysis of brewing industry wastes. *Waste Manag.* **2020**, *113*, 96–104. [[CrossRef](#)]
39. Massardi, M.M.; Massini, R.M.M.; De Silva, D.J. Chemical characterization of brewer's spent grains and evaluation of its potential for obtaining value-added products. *J. Eng. Exact Sci.* **2020**, *6*, 0083–0091. [[CrossRef](#)]
40. Coutinho, N.C.; Vieira, C.M.F. Characterization and incorporation of MSWI ash in red ceramic. *Cerâmica* **2016**, *62*, 249–255. (In Portuguese) [[CrossRef](#)]
41. Pedroti, L.G.; Alexandre, J.; Xavier, G.C.; Monteiro, S.N.; Vieira, C.M.F.; Bahiense, A.V.; Maia, P.C.A. Development of ceramic mass for fired and pressed blocks. *Cerâmica Ind.* **2011**, *16*, 25–30. (In Portuguese)
42. Silva, A.M.F.D. Incorporation of Elephant Grass Ash in Red Ceramic. Master's Thesis, Graduate Program in Engineering and Materials Science. University of North Fluminense, Campos dos Goytacazes, Rio de Janeiro, Brazil, 2015. (In Portuguese).
43. Vieira, C.M.F.; Soares, T.M.; Monteiro, S.N. Ceramic bodies for roofing tiles: Characteristics and firing behavior. *Cerâmica* **2003**, *49*, 245–250. (In Portuguese) [[CrossRef](#)]
44. Ribeiro, S.; Strecker, K.; Vernilli, F., Jr. Use of dilatometry to study the effect of different additives on the sintering of Si_3N_4 . *Cerâmica* **2000**, *46*, 34–39. (In Portuguese) [[CrossRef](#)]
45. Tubino, L.C.B.; Borba, P. *Technical Dossier: Stages of the Ceramic Process and Its Influence on the Final Product—Mass, Extrusion, Drying and Firing*; SENAI: Rio Grande do Sul, Brazil, 2006; pp. 1–19. (In Portuguese)
46. Luiz, N.F. Evaluation of the Use of Ornamental Rock Residue in the Incorporation of Ceramic Mass for the Manufacture of Tiles. Master's Thesis, Department of Agricultural and Environmental Engineering, Graduate Program in Biosystems Engineering, Federal Fluminense University, Rio de Janeiro, Brazil, 2019. (In Portuguese).
47. Meneses, M.J.S. Calorific Power and Immediate Analysis of Pine (*Pinus* sp.) and Araucaria (*Araucaria angustifolia*) Wood Shavings from Reforestation as Timber Waste. Master's Thesis, Graduate Program in Energy in Agriculture, State University of West Paraná, Cascavel, Paraná, 2013; pp. 65p. (In Portuguese).
48. Cotes-Palomino, M.T.; Martínez-García, C.; Eliche-Quesada, D.; Pérez-Villarejo, L. Production of ceramic material using wastes from brewing industry. *Key Eng. Mater.* **2016**, *663*, 94–104. [[CrossRef](#)]
49. Russ, W.; Mörtel, H.; Meyer-Pittroff, R. Application of spent grains to increase porosity in bricks. *Constr. Build. Mater.* **2005**, *19*, 117–126. [[CrossRef](#)]
50. Silva, T.R.; Cecchin, D.; Azevedo, A.R.G.; Alexandre, J.; Valadão, I.C.R.P.; Bernardino, N.A.; Carmo, D.F.; Ferraz, P.F.P. Soil-cement blocks: A sustainable alternative for the reuse of industrial solid waste. *Braz. J. Environ. Sci.* **2021**, *56*, 673–686. [[CrossRef](#)]
51. *NBR 15270-1*; Eramic Components—Blocks and Bricks for Masonry—Part 1: Requirements. Brazilian Association of Technical Standards—ABNT: Rio de Janeiro, Brazil, 2017. (In Portuguese)
52. *NBR 15310*; Amendment 1:2009: Ceramic Components—Tiles—Terminology, Requirements and Test Methods. Brazilian Association of Technical Standards—ABNT: Rio de Janeiro, Brazil, 2009. (In Portuguese)
53. Cargnin, M.; Souza, S.M.A.G.U.; Souza, A.A.U.; Noni, A., Jr. Determination of kinetic parameters of sintering of ceramic type BIIa single firing. *Cerâmica* **2011**, *57*, 461–466. [[CrossRef](#)]
54. Ketov, A.; Rudakova, L.; Vaisman, I.; Ketov, I.; Haritonovs, V.; Sahmenko, G. Recycling of rice husks ash for the preparation of resistant, lightweight and environment-friendly fired bricks. *Constr. Build. Mater.* **2021**, *302*, 124385. [[CrossRef](#)]

Disclaimer/Publisher's Note: The statements, opinions and data contained in all publications are solely those of the individual author(s) and contributor(s) and not of MDPI and/or the editor(s). MDPI and/or the editor(s) disclaim responsibility for any injury to people or property resulting from any ideas, methods, instructions or products referred to in the content.